Journal of Biomolecular NMR, 1 (1991) 145–154
ESCOM

J-Bio NMR 004

Comparison of amide proton exchange in reduced and oxidized *Rhodobacter capsulatus* cytochrome c_2: A ^1H-^{15}N NMR study

Paul R. Gooley, Dezheng Zhao and Neil E. MacKenzie*

Department of Pharmaceutical Sciences, College of Pharmacy, University of Arizona, Tucson, AZ 85721, U.S.A.

Received 17 December 1990
Accepted 10 January 1991

Keywords: NMR; Cytochrome; Dynamics; Amide exchange

SUMMARY

The hydrogen-deuterium exchange rates of the reduced and oxidized forms of *Rhodobacter capsulatus* cytochrome c_2 were studied by ^1H-^{15}N homonuclear multiple quantum correlation spectroscopy. Minimal differences were observed for the N- and C-terminal helices on changing redox state suggesting that although these helices are structurally important they do not affect the relative stability of the two redox states and hence may not be important in determining the redox potential differences observed amongst the class I c-type cytochromes. However, significant differences were observed for other regions of the protein. For example, all slow exchanging protons of the helix spanning Phe^{82} to Asp^{87} are similarly affected on reduction indicating that the unfolding equilibrium of this helix is altered between the two redox states. Other regions are not as simple to interpret; however, the difference in NH exchange rates between the redox states for a number of residues including His^{17}, Leu^{37}, Arg^{43}, Ala^{45}, Gly^{46}, Ile^{57}, Val^{58}, Leu^{60}, Gly^{61} and Leu^{100} suggest that interactions affecting the causes of these differences may be important factors in determining redox potential.

INTRODUCTION

The class I c-type cytochromes present an interesting problem in the study of protein function, and that is to elucidate which properties of the protein determine the magnitude of the oxidation-reduction potential. Although there is minimal amino acid sequence homology in this class of cy-

Abbreviations: NMR, nuclear magnetic resonance; HMQC, homonuclear multiple quantum correlation; NOESY, nuclear Overhauser effect spectroscopy.

* To whom correspondence should be addressed.

tochromes, significant structural homology is observed between the individual members (Cusanovich et al., 1988). For example, all members have N- and C-terminal helices, Met and His as extraplanar heme ligands and two Cys residues, near the N-terminal helix, which form thioether bonds with the heme. The protein fold results in a hydrophobic environment around the heme to give these cytochromes a positive reduction potential, and thus favoring electron retention (Kassner, 1972). The structure of at least 11 class I c-type cytochrome have been determined (Cusanovich et al., 1988; Louie and Brayer, 1990; Bushnell et al., 1990). Comparison of accurate structures for reduced (tuna and yeast) and oxidized (tuna and rice) states show no significant shifts in the main-chain atoms on changing redox state (Takano and Dickerson, 1981b; Louie and Brayer, 1990). For tuna cytochrome c there are subtle structural changes of 0.1 to 0.7 Å of side-chain atoms between the redox states that, most importantly, involve the approach of a water molecule to the heme iron and a greater degree of exposure of the heme to solvent in the oxidized form (Takano and Dickerson, 1981b). Although this behavior may be common to a number of class I c-type cytochromes their redox potentials range from about 20 to 500 mV (Cusanovich et al., 1988) suggesting that some nonconserved residues have an important function in controlling redox potential. The function of these residues may be to enhance the hydrophobic difference of the heme environment between the two redox forms.

The subtle structural changes that occur between reduced and oxidized cytochromes c are accompanied by pronounced changes in protein stability. A number of chemical properties of the horse cytochrome c, such as pH dependence, surface denaturation, thermal resistance and protease digestion, show that the oxidized form is less stable than the reduced form of cytochrome c (Dickerson and Timkovich, 1975). Therefore the heme exposure in the oxidized form can be thought of as a shift in the equilibrium towards the ensemble of unfolded conformers and thus, the role of the residues that are determining the difference in redox potential of the cytochromes may mediate this dynamic control. Differences in the folding equilibrium of the oxidized and reduced cytochromes c can be qualitatively measured by hydrogen-deuterium exchange rates of the NH protons that stabilize secondary and tertiary structure by hydrogen bonds (Wand et al., 1986). These exchange rates may, in turn, relate to the molecular factors that determine redox potential.

In this paper we present an analysis of the solvent hydrogen-deuterium exchange of the NH protons of cytochrome c_2 from *Rhodobacter capsulatus*, a member of the class I c-type cytochromes. The backbone ^1H and ^{15}N NMR assignments of both the reduced and oxidized forms have been completed (Gooley et al., 1990; Zhao et al., unpublished). Our present objective is to determine the extent and magnitude of differences in hydrogen-deuterium exchange rates of the two redox states as a guide to construct cytochrome c_2 mutants that show substantial differences in redox potential and thus understand the determinants of this important physiological phenomenon.

MATERIALS AND METHODS

The preparation and purification of ^{15}N-enriched cytochrome c_2 with $(^{15}NH_4)_2SO_4$ (Isotech, Inc.) has been described previously (Gooley et al., 1990). Samples of cytochrome c_2 were reduced or oxidized with several crystals of sodium dithionite or potassium ferricyanide, respectively. The reductant and oxidant were subsequently removed by repeated ultrafiltration at 4°C. Hydrogen-

deuterium exchange was initiated by concentrating the samples three times with 0.5 to 1 ml aliquots of 50 mM phosphate, D_2O and pH 6 at 4°C. 2 mM dithiothreitol was added to the buffer of the reduced protein. Prior to capping the NMR tube samples were flushed with argon.

The experimental procedure for acquiring and processing ^1H-^{15}N HMQC to obtain hydrogen-deuterium NH exchange rates was similar to a previous report (Gooley et al., 1990). Samples were exchanged with the above D_2O buffer for 40 min at 4°C then placed in the spectrometer. After 10 min of temperature equilibration at 30°C the first spectrum was acquired. ^1H-^{15}N HMQC spectra (Bax et al., 1983) were acquired with spectral widths of 5000 Hz (^1H) and 2000 Hz (^{15}N) and 100 t_1 points. Acquisition times of 24 min (8 scans, 2 dummy scans) were used for spectra up to 1000 min of exchange and 38 min (16 scans, 2 dummy scans) between 1000 and 80000 min of exchange. Reduced samples were reequilibrated with fresh buffer every 8 days. The experiment with the oxidized sample lasted 7000 min and therefore was not reequilibrated.

Spectra were processed on a VAX 8600 using FTNMR (Hare Research). Prior to 2D Fourier transformation the data were multiplied by shifted sine bells in both t_1 and t_2, and zerofilled to yield a matrix of 1024 × 1024 real data points. In the course of ongoing hydrogen-deuterium exchange experiments, peak volumes have been calculated manually by two methods. The first method uses the subcommand 't' assuming an elliptical peak shape. The second method uses the subcommand 'i' and thus a square foot print, where the radius was equal to half the peak width at the base of the peak in the ^1H dimension. The first method proved unsatisfactory where peaks overlap or are not well resolved, whereas the second method did not calculate the total peak volume. Rate constants derived from either method were, generally, not significantly different. As the second method allows calculation of rate constants for almost all the peaks, except those that are coincident, this method is preferred. One-dimensional amide exchange studies of the reduced and oxidized cytochrome c_2 showed that the intensity of the resolved N(1)H of Trp^{67} does not change after 80000 and 7000 min, respectively, of exchange, therefore this resonance was used as an internal standard. During these studies of reduced cytochrome c_2 the exchange rate constant of the resolved $N_\pi H$ of His^{17} was calculated to be $0.58 \times 10^{-5}\ min^{-1}$ (Gooley and MacKenzie, 1990). The rate constant of this proton in the two-dimensional studies of reduced cytochrome c_2 is calculated to be $0.62 \times 10^{-5}\ min^{-1}$, thus serving as an additional check on the methods of calculation. Rate constants were calculated by exponential least-squares analysis of plots of $I = Ae^{-kmt}$, where I is the measured peak volume, A the initial peak volume, k_m the exchange rate constant (min^{-1}) and t is time (min). All measured peak volumes were used in the calculation, and assuming single exponentials the estimated standard deviations for k_m were less than ± 10%.

NOESY spectra (Jeener et al., 1979) of *R. capsulatus* ferrocytochrome c_2 were acquired at pH 6 and 30° or 40°C with a spectral width of 10000 Hz, 900 t_1 points, 2K data points in t_2 and 96 to 128 transients for each t_1 point and mixing times of 50 or 100 ms. Spectra were processed as above, but were zero-filled to yield spectra of 2048 × 2048 real data points.

RESULTS AND DISCUSSION

Mechanism of hydrogen-deuterium exchange

The measured hydrogen-deuterium exchange of an NH proton for a solvent deuteron can be expressed in the following scheme (Hvidt and Nielsen, 1966):

$$N(H) \underset{k_u}{\overset{k_f}{\rightleftharpoons}} O(H) \xrightarrow[D_2O]{k_c} O(D) \underset{k_f}{\overset{k_u}{\rightleftharpoons}} N(D) \quad (1)$$

where N is the native state and O includes all the open states of the protein, k_c, k_u and k_f are the intrinsic rate (Molday et al., 1972), unfolding and refolding constants, respectively. In this model hydrogen-bond breakage occurs by localized unfolding events rather than single bonds and thus at a given time there would be a small concentration of a large variety of open states (Englander and Kallenbach, 1983). A second model proposes solvent penetration into the protein by diffusion through channels opened by small atomic fluctuations (Englander and Kallenbach, 1983). This model would suggest that the relative position of an NH proton to the protein surface would be rate-limiting. Although solvent accessibility is important, a significant body of data suggests that relative access does not determine the exchange rate (Wagner and Wüthrich, 1982; Kuwajima and Baldwin, 1983; Wand et al., 1986).

From scheme 1 if $k_f \gg k_u$ the experimentally measured NH exchange rate constant, k_m, is (Hvidt and Nielsen, 1966):

$$k_m = (k_u \cdot k_c)/(k_f + k_c) \quad (2)$$

Under most experimental conditions hydrogen exchange in stable proteins occurs in the EX2 limit, where $k_c \ll k_f$ is limiting (Roder et al., 1985), thus:

$$k_m = (k_u/k_f)k_c = K_{op} \cdot k_c \quad (3)$$

where K_{op} is the local unfolding equilibrium constant. As previously noted (Wand et al., 1986) the free energy difference ΔG_{op} between the open and closed forms can be calculated from K_{op}:

$$\Delta G_{op} = -RT\ln(K_{op}) \quad (4)$$

Comparing differences for respective exchange rates in two forms of a protein, for example, between oxidized and reduced cytochrome c_2 or mutant proteins, changes in K_{op} result in changes in free energy differences:

$$\delta\Delta G_{op} = -RT\ln(\delta K_{op}) = -RT\ln(k_m^1/k_m^2) \quad (5)$$

where k_m^1 and k_m^2 are the exchange rates for the same NH proton in two forms of the protein. In this idealized situation an assumption has been made. For exchange to occur in the open states with a rate k_c requires near complete unfolding. If this state is not achieved, providing the exchange of respective protons occurs in the same unfolded conformation for the two forms of the protein, $\delta\Delta G_{op}$ will report differences in only the unfolding equilibria. However, if these unfolded states differ, exchange will occur by different apparent intrinsic rate constants, k_c^{app1} and k_c^{app2}, where $k_c^{app1} \neq k_c^{app2} < k_c$. Such conditions include changes to relative solvent access and differences in the structure of the open state. Therefore values of $\delta\Delta G_{op}$ are limited to a qualitative interpretation, but are significant in that they may point to functionally important regions of the protein.

NH Exchange and free energy differences of oxidized and reduced R. capsulatus *cytochrome* c_2

The exchange rates of NH protons with half-lives of 50 min or greater at pH 6 and 30°C for the reduced and oxidized cytochrome c_2 are shown in Fig. 1. From these rates, $\delta\Delta G_{op}$ (ΔG_{op} of reduced less ΔG_{op} of oxidized cytochrome c_2) were calculated by Eq. 5 and are plotted in Fig. 2. There appears to be a minimal $\delta\Delta G_{op}$ of 0.2 kcal · mol^{-1}, except for Ala^{112} which shows a $\delta\Delta G_{op}$ of -0.2 kcal · mol^{-1}. Although these changes are within experimental error, which is estimated to be ± 0.5 kcal · mol^{-1}, the minimal loss of stability for the oxidized cytochrome c_2 may represent the difficulty in maintaining the oxidized sample. However, during the 7000 min of this latter experiment, one-dimensional spectra of the oxidized sample were acquired and show less than a 10% contamination of reduced cytochrome c_2.

The secondary structure of reduced *R. capsulatus* cytochrome c_2 has been determined from the analysis of the sequential and short-range NOESY data (Gooley et al., 1990). Determination of the global fold of this protein by two-dimensional NMR has proved difficult, in part, due to the problem of obtaining complete and unambiguous assignment of all NOEs. However, we have assigned 478 sequential and short-range and 235 long-range NOEs. While these data are not sufficient for the calculation of a solution structure of reasonable quality, the apparent global fold is, as expected, similar to other class I c-type cytochromes (Takano and Dickerson, 1981a; Bhatia, 1981; Bushnell et al., 1990; Louie and Brayer, 1990). A number of pertinent long-range NOEs that verify this global fold are shown in Fig. 3 and are described throughout the following discussion. To assist in the understanding of the NH exchange data a model of the *R. capsulatus* cytochrome c_2 based on the crystal coordinates of another class I c-type cytochrome c, *Rhodospirillium rubrum* cytochrome c_2 (Bhatia, 1981), is presented in Fig. 4.

A striking observation is that the N- and C-terminal helices, spanning Ala^3 to Cys^{13} and Gly^{103}

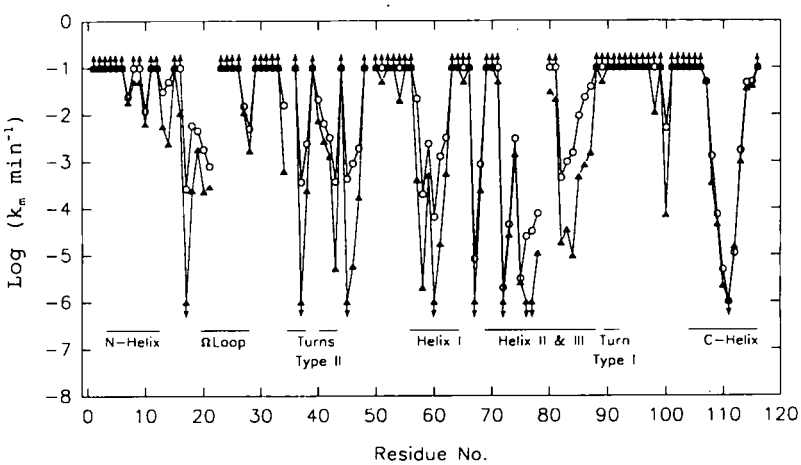

Fig. 1. Plot of log(k_m min^{-1}) versus amino acid sequence number of reduced (▲) and oxidized (o) *R. capsulatus* cytochrome c_2, pH 6 and 30°C. Standard deviations of k_m are $\pm 10\%$. Arrows indicate the rate is faster (↑) or slower (↓) than indicated. The ^{1}H-^{15}N correlations of Gly^{42} and Leu^{83} in oxidized cytochrome c_2 are degenerate. The data for this peak fits a single exponential and the rate determined ($0.97 \pm 0.04 \times 10^{-3}$ min^{-1}) is slightly slower than the rate for Gly^{42} in reduced cytochrome c_2. Therefore the calculated rate is assigned to Leu^{83} and is estimated for Gly^{42}. Elements of secondary structure are indicated (Gooley et al., 1990).

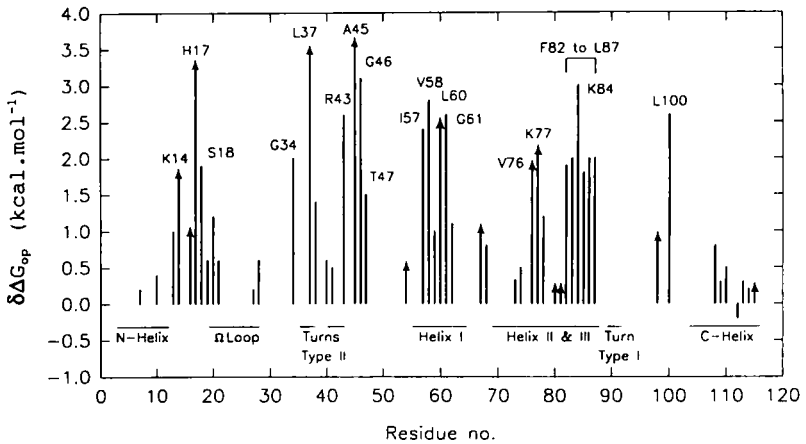

Fig. 2. Plot of apparent $\delta\Delta G_{op}$ versus amino acid sequence number of reduced and oxidized *R. capsulatus* cytochrome c_2, pH 6 and 30°C. Arrows (↑) indicate that $\delta\Delta G_{op}$ is underestimated and are shown for residues where a rate was obtained for one form of the protein but not the other. Elements of secondary structure are indicated (Gooley et al., 1990).

to Val^{115}, respectively, show only small $\delta\Delta G_{op}$. Previous analysis of NOE data shows that the N-terminal helix in this cytochrome c_2 is distorted and extends to His^{17} (Gooley et al., 1990). However, other class I c-type cytochromes (Takano and Dickerson, 1981a; Bhatia, 1981; Bushnell et al., 1990; Louie and Brayer, 1990) show that the analogous and conserved region Cys^{13} to His^{17} is not a part of this helix. Therefore the N-terminal helix probably spans Ala^3 to Cys^{13}. The exchange rates of the NH protons for this distorted helix are fast compared to the other four helices of this cytochrome c_2 and to those of the N-terminal helix of horse cytochrome c (Wand et al., 1986). However, in this helix there are two NH protons, Glu^7 and Phe^{10}, with measurable exchange rates in both reduced and oxidized cytochrome c_2. For these protons $\delta\Delta G_{op}$ is calculated to be 0.2 and 0.4 kcal · mol^{-1}, respectively (Fig. 2). These differences are not considered significant and therefore indicate that the local folding equilibrium of the N-terminal helix is the same in both reduced and oxidized cytochrome c_2. Note that this behavior is similar to that of the N-terminal helix of horse cytochrome c (Wand et al., 1986). $\delta\Delta G_{op}$ for the NH protons in the C-terminal helix of *R. capsulatus* cytochrome c_2, spanning the segment Ala^{109} to Val^{114}, are shown in Fig. 2, and range from −0.2 to 0.5 kcal · mol^{-1} while the NH proton of Ala^{108} shows a difference of 0.8 kcal · mol^{-1}. With the exception of the latter value these differences are not significant suggesting that the folding equilibrium for this helix is the same for reduced and oxidized cytochrome c_2. From these data we conclude that while the N- and C-terminal helices are structurally important to the protein, they may not play a role in controlling redox potential or in the dynamic properties of the two redox states. Interestingly, the N- and C-terminal helices are proximal to each other as indicated by long-range NOEs, for example, from NH of Gly^6 to βH_2 of Asp^{106} and from the ring of Phe^{10} to the methyl groups of Leu^{111} (Figs. 3A and D; Fig. 4).

Twenty two NH protons show large $\delta\Delta G_{op}$, ranging between 1.5 to 3.5 kcal · mol^{-1} (Fig. 2). NOEs suggest that these protons are from several regions. Five of these, Arg^{43}, Ala^{45}, Gly^{46}, Thr^{47} and Ile^{57} form a cluster near Trp^{67} (Fig. 4). Another five, Lys^{14}, His^{17}, Ser^{18}, Gly^{34} and Leu^{37} form another cluster after the C-terminus of the N-terminal helix (Gooley et al., 1990). The three residues, Val^{58}, Leu^{60} and Gly^{61}, stabilize the short central helix (helix I) spanning Asp^{55} to

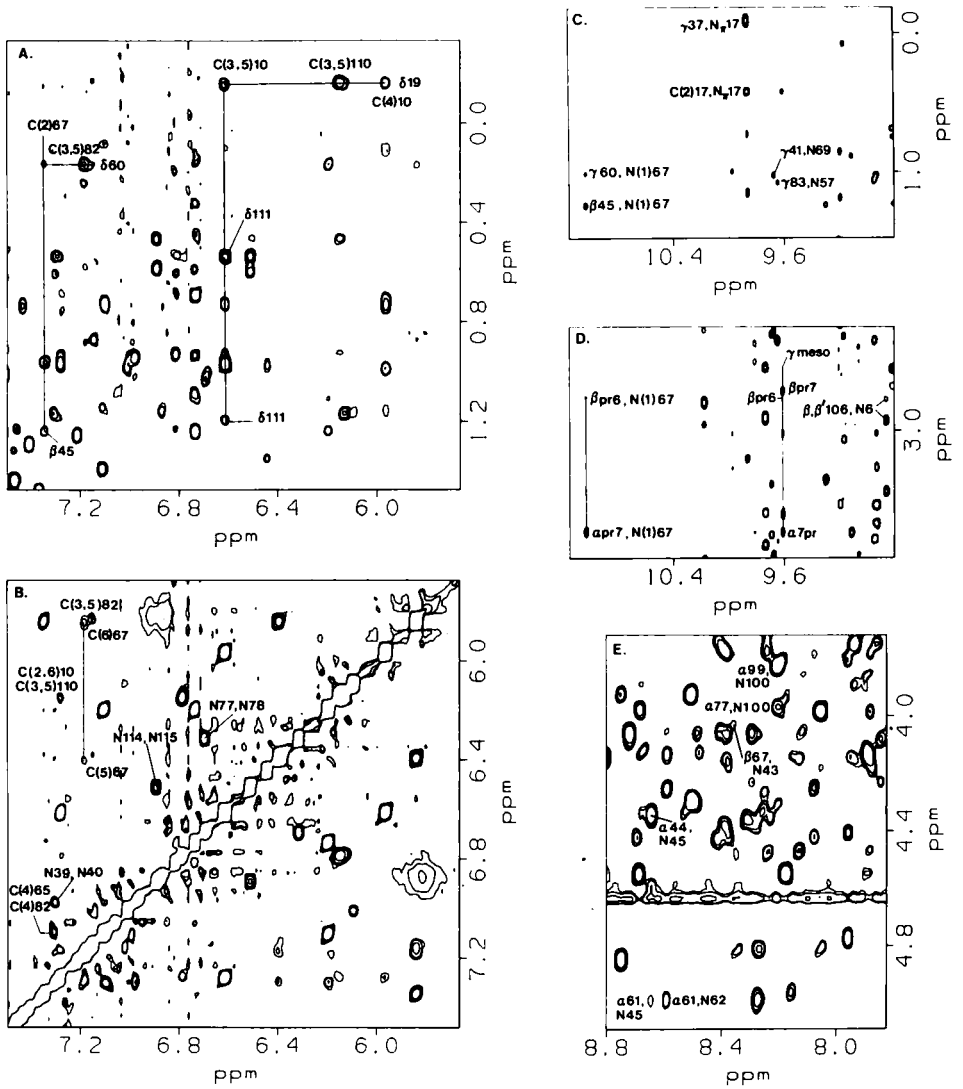

Fig. 3. Sections of a NOESY spectrum of *R. capsulatus* ferrocytochrome c_2, pH 6 and 40°C recorded with a mixing time of 50 ms. Pertinent long-range NOEs that indicate the global fold of this cytochrome c_2 is similar to other class I c-type cytochromes are described. βpr6,αpr7 and βpr7 indicate connectivities to the α and β propionate-6 and -7 protons; γmeso is the γ-meso proton of the heme.

Phe^{65}. Another eight residues, Val^{76} and Lys^{77} and the segment Phe^{82} to Leu^{87}, belong to the two helices separated by Pro^{79} and which span Glu^{69} to Asp^{78} (helix II) and Phe^{82} to Asp^{88} (helix III), respectively (Gooley et al., 1990). NOEs from the NH of Leu^{100} to the αH of Lys^{77} (Fig. 3E) and from the εH_3 of Met^{96} to the γH_3 of Val^{76} suggest that the NH of the remaining residue, Leu^{100}, is near helix II (Fig. 4). Interestingly, NOEs from the NH of Ala^{45} to the αH of Gly^{61} (Fig. 3E), the NH of Ile^{57} to a γH of Leu^{83} (Fig. 3C), a δH_3 of Leu^{60} to the C(3,5)H of Phe^{82} (Fig. 3A), the C(4)H of Phe^{65} to the C(4)H of Phe^{82} (Fig. 3B), and both C(5)H and C(6)H of Trp^{67} to C(3,5)H of Phe^{82} (Fig. 3B) indicate that helix I is proximal to both the cluster near Trp^{67} and to helix III (Fig. 4).

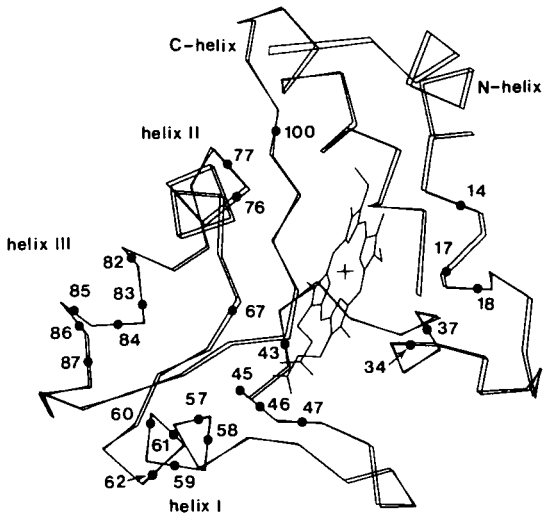

Fig. 4. Ribbon model of *R. capsulatus* cytochrome c_2 based on the X-ray crystal coordinates of *R. rubrum* cytochrome c_2 (Bhatia, 1981). NH protons that show exchange rate constant differences for reduced versus oxidized *R. capsulatus* cytochrome c_2 are indicated. The probable location of Trp^{67} is also indicated.

Similar hydrogen-deuterium exchange rate values for helical segments, irrespective of their position to the protein surface, suggest that hydrogen-bond breakage occurs in cooperative unfolding units (Wagner and Wüthrich, 1982; Englander and Kallenbach, 1983; Wand et al., 1986). Additional evidence of such a phenomenon would be a perturbation of the unfolding equilibria of these units of structure and thus a similar change in rates of NH exchange (Englander et al., 1983). Apparent uncooperative exchange may be due to changes in structure, solvent accessibility or separate folding units. Although there is some correlation between the degree of slowing of hydrogen-deuterium exchange and the relative position of the NH proton to the surface of cytochrome c_2 the exchange rate differences and $\delta\Delta G_{op}$ for residues Phe^{82} to Leu^{87} of helix III are strikingly similar asserting that these residues belong to a single cooperative unfolding unit (Figs. 1 and 2). These six residues span almost two turns of the helix which suggests that residues are distributed on both the surface and in the interior of the protein (Fig. 4). Therefore, the position of the residue does not appear to influence $\delta\Delta G_{op}$. For Lys^{84}, $\delta\Delta G_{op}$ is 3.0 kcal · mol^{-1} which is 1 kcal · mol^{-1} more than $\delta\Delta G_{op}$ for the other residues suggesting that the NH exchange of this proton may be affected by both a change in unfolding equilibria and in relative solvent accessibility. The NH protons of Val^{58} to Ala^{62} stabilize helix I. Val^{58}, Leu^{60} and Gly^{61} show $\delta\Delta G_{op}$ of 2.8, 2.5 and 2.6 kcal · mol^{-1}, respectively, while Ala^{59} and Ala^{62} show $\delta\Delta G_{op}$ of 1.0 and 1.1 kcal · mol^{-1}. These differences suggest that either this folding unit is not cooperative or that changes to solvent accessibility or to structure are present. Interestingly, the position of these residues within the helix indicate that Val^{58}, Leu^{60} and Gly^{61} are on a different face of the protein than Ala^{59} and Ala^{62} where possibly the former groups are in the interior and the latter are on the protein surface (Fig. 4) suggesting that, in this case, solvent accessibility may be the predominant factor. In helix II, Val^{76}, Lys^{77} and Asp^{78} show $\delta\Delta G_{op}$ of 1.2 to more than 2.0 kcal · mol^{-1}, while Ala^{73} and Thr^{74} show $\delta\Delta G_{op}$ of 0.3 to 0.5 kcal · mol^{-1}. These differences suggest that there may also be a structural or a solvent-accessibility change to the segment spanning Val^{76} to Asp^{78} or that helix II consists

of more than one unfolding unit. Comparisons to the hydrogen-bond network of other class I c-type cytochromes (Takano and Dickerson, 1981a; Bhatia, 1981; Bushnell et al., 1990; Louie and Brayer, 1990) and long-range NOE data further suggest that the NH of Leu^{100} is hydrogen bonded to the carbonyl of Val^{76}, and therefore $\delta\Delta G_{op}$ for Leu^{100} may be due to the same phenomena affecting Val^{76} to Asp^{78}.

The dynamics of the oxidation state of cytochrome c_2

The exchange rate data suggests that the unfolding equilibria of helix III differ for the two oxidation states. However, it is difficult to conclude whether the NH exchange differences for the other NH protons are due to unfolding equilibria or solvent accessibility and this requires detailed knowledge of the structure of both oxidation states. Irrespective of the reasons for the increase in exchange rates, there appears to be a generalized effect to the dynamics of the protein that involves the lower left-hand-side portion of the cytochrome c_2 (Fig. 4). The structures of both oxidation states of tuna cytochrome c are available and show only small shifts of less than 0.7 Å within the analogous region (Takano and Dickerson, 1981b). Although we do not expect differences to be any greater in *R. capsulatus* cytochrome c_2, structural shifts of approximately 1 Å may be sufficient to cause variations of up to 10^2 for the NH exchange rates by altering hydrogen bond lengths and thus, destabilizing structural elements.

The changes observed may be due to many complex interactions between backbone, side chain, heme, bound water and the solvent. Detailed examination of NOESY spectra of reduced cytochrome c_2 shows that His^{17} interacts with Gly^{34} and Leu^{37} (Fig. 3C; Gooley et al., 1991), the segment Ala^{45} to Thr^{47} with helix II, for example Ala^{45} to Gly^{61} (Fig. 3E) and helix II with helix III, for example Ile^{57} to Leu^{83} (Fig. 3C) and Phe^{65} to Phe^{82} (Fig. 3B). For tuna cytochrome c, the movement of several side chains and an internal water molecule may be a key component to determining the redox potential of this cytochrome (Takano and Dickerson, 1981b). A similar water molecule remains to be located in *R. capsulatus* cytochrome c_2. However, this study indicates that the two helices I and III are more open or unfolded in the oxidized than the reduced cytochrome c_2 which may increase the solvent exposure of the heme.

The largest $\delta\Delta G_{op}$ that are obtained in this study are His^{17} (> 3.3 kcal $\cdot$ mol^{-1}), Leu^{37} (> 3.5), Ala^{45} (> 3.6), Gly^{46} (3.1) and Lys^{84} (3.0). These values are surprisingly similar to the global free-energy difference of 3.7 ± 0.4 kcal $\cdot$ mol^{-1}, determined by solvent denaturation experiments based on the change in the helix circular dichroism signal at 220 nm, pH 7.5 and 25°C (Caffrey, 1990). It is important to consider both hydrogen bond partners, particularly in the tertiary structure, when attempting to understand changes to the dynamics and structure of a protein. Comparison to other class I c-type cytochromes suggests the following hydrogen bonds (Takano and Dickerson, 1981a; Bhatia, 1981; Bushnell et al., 1990; Louie and Brayer, 1990): His^{17} to Cys^{13}, Leu^{37} to Ser^{18}, Ala^{45} to Phe^{65}, Gly^{46} to propionate-7 and Lys^{84} to Gly^{80}. Figure 4 shows that these residues and their partners are not a part of a localized region, but two or three regions. One region involves Cys^{13}, His^{17}, Ser^{18} and Leu^{37} and another Ala^{45}, Gly^{46}, Phe^{65} and propionate-7. As the helices that contain Phe^{65} and Lys^{84} interact, Lys^{84} and Gly^{80} may be a part of the latter region. These data suggest that at least two apparently non-interacting regions are affected by the change in redox state. However, key interactions such as the movement of side chains and changes to heme ligand bonds may tie these regions together.

This study serves as a guide from a dynamics rather than a structural perspective in searching for key factors that control redox potential. Our hypothesis is that mutations that alter the redox potential will change the hydrogen-deuterium exchange rates of one or more of the regions identified in this study. Of the 22 NH protons that show large $\delta\Delta G_{op}$ (> 1.5 kcal $\cdot$ mol^{-1}), His^{17}, Ser^{18}, Gly^{34}, Leu^{37}, Arg^{43}, Gly^{46}, Val^{76}, Phe^{82}, Leu^{83}, Glu^{85} and Leu^{100} are highly conserved and, except for His^{17} and Ser^{18}, the expected partner of the hydrogen bond is highly conserved, for example, Gly^{34}(NH) to Cys^{16}(CO), Leu^{37}(NH) to Ser^{18}(CO) and Arg^{43}(NH) to Val^{40}(CO) (Takano and Dickerson, 1981a; Bhatia, 1981; Bushnell et al., 1990; Louie and Brayer, 1990). The 11 remaining NH protons are not conserved, and we can only comment on the situation where the hydrogen bond is highly conserved in other class I c-type cytochromes, but the partners are not; for example, Val^{58}, Leu^{60} and Gly^{61} of helix I and Ala^{81}, Lys^{84}, Lys^{86} and Leu^{87} of helix III are all poorly conserved. Mutations within these regions may further enlarge our understanding of why these hydrogen bonds are conserved and the importance of the individual residues as determinants of the redox potential.

ACKNOWLEDGEMENTS

This work was supported in part by the Arizona Research Laboratories Division of Biotechnology and by grants BRSGS07-RR07002 and RR05605 from the National Institutes of Health. We thank Ms Ellie Nielson for technical assistance and protein purification; Drs Michael Caffrey and Michael Cusanovich for helpful and meaningful discussions and Dr Hazel Holden for making available the X-ray crystal coordinates of *R. capsulatus* cytochrome c_2 prior to publication.

REFERENCES

Bax, A., Griffey, R.H. and Hawkins, B.L. (1983) *J. Magn. Reson.*, **55**, 301-315.
Bhatia, G.E., (1981) Ph.D. Thesis, University of California, San Diego.
Bushnell, G.W., Louie, G.V. and Brayer, G.D. (1990) *J. Mol. Biol.*, **214**, 585-595.
Caffrey, M.S. (1990) Ph.D. Thesis, University of Arizona, Tucson.
Cusanovich, M.A., Meyer, T.E. and Tollin, G. (1988) In *Advances in Inorganic Biochemistry, Heme Proteins 7*, (Eds, Eichhorn, G. L. and Manzilli, L. G.) Elsevier, New York, pp. 37-92.
Dickerson, R.E. and Timkovich, R. (1975) in *The Enzymes*, 3rd ed., Vol. 11 (Ed, Boyer, P.D.), Academic Press, N.Y., pp. 397-547.
Englander, J.J., Rogero, J.R. and Englander, S.W. (1983) *J. Mol. Biol.*, **169**, 325-344.
Englander, S.W. and Kallenbach, N.R. (1984) *Q. Rev. Biophys.*, **16**, 521-655.
Gooley, P.R., Caffrey, M.S., Cusanovich, M.A. and MacKenzie, N.E. (1990) *Biochemistry*, **29**, 2278-2290.
Gooley, P.R. and MacKenzie, N.E. (1990) *FEBS Lett.*, **260**, 225-228.
Gooley, P.R., Caffrey, M.S., Cusanovich, M.A. and MacKenzie, N.E. (1991) *Eur. J. Biochem.*, **196**, 653-661.
Hvidt, A. and Nielsen, S.O. (1966) *Adv. Protein Chem.*, **21**, 287-386.
Jeener, J., Meier, B.H., Bachman, P. and Ernst, R.R. (1979) *J. Chem. Phys.*, **71**, 4546-4553.
Kassner, R.J. (1972) *Proc. Natl. Acad. Sci. USA*, **69**, 2263-2267.
Kuwajima, K. and Baldwin, R.L. (1983) *J. Mol. Biol.*, **169**, 299-323.
Louie, G.V. and Brayer, G.D. (1990) *J. Mol. Biol.*, **214**, 527-555.
Molday, R.S., Englander, S.W. and Kallen, R.G. (1972) *Biochemistry*, **11**, 150-158.
Roder, H., Wagner, G. and Wüthrich, K. (1985) *Biochemistry*, **24**, 7396-7407.
Takano, T. and Dickerson, R.E. (1981a) *J. Mol. Biol.*, **153**, 79-94.
Takano, T. and Dickerson, R.E. (1981b) *J. Mol. Biol.*, **153**, 95-115.
Wagner, G. and Wüthrich, K. (1982) *J. Mol. Biol.*, **160**, 343-361.
Wand, A.J., Roder, H. and Englander, S.W. (1986) *Biochemistry*, **25**, 1107-1114.